WORLD JOURNAL OF PHARMACEUTICAL RESEARCH
SJIF Impact Factor 7.523
Volume 7, Issue 8, 122-135. Conference Article ISSN 2277– 7105

SYNTHESIS, STRUCTURAL, OPTICAL AND THERMAL PROPERTIES OF PURE AND GD^{3+} DOPED MNWO4 COMPOUNDS

P. Prabukanthan*, R. Aswini and S. Niresh Babu

Materials Chemistry Lab, Department of Chemistry, Muthurangam Government Arts College, Vellore 632 002, India.

Article Received on
05 March 2018,
Revised on 25 March 2018,
Accepted on 15 April 2018
DOI: 10.20959/wjpr20188-10938

***Corresponding Author**
P. Prabukanthan
Materials Chemistry Lab, Department of Chemistry, Muthurangam Government Arts College, Vellore 632 002, India.

ABSTRACT

Pure and Gd^{3+} doped manganese tungstate ($MnWO_4$) compounds semiconductors were prepared by solid-state metathetic approach assisted microwave irradiation using sodium tungstate ($Na_2WO_4{\cdot}2H_2O$), $Gd(CH_3COO)_3$ and $MnCl_2$ solutions as precursors. The morphology and crystal phase of the as-synthesised pure and Gd^{3+} doped manganese tungstate were characterized by scanning electron microscopy (SEM) and X-ray diffraction (XRD) analysis. The above characterizations render that the products obtained belong to the wolframite-like monoclinic crystal system, with average size of cuboid nanoparticles about 150 nm to 300 nm in the pure Gd^{3+} doped $MnWO_4$. In the diffuse reflectance UV-Visible absorption spectra shows that the strong absorption maximum of ~359 nm was observed for pure and Gd^{3+} doped $MnWO_4$. Due to the high crystallinity the samples have shown more prominent UV absorption maxima. The strong band located at about 359 nm can be assigned to the intense band to band transition corresponding to the absorption between the O 2p level and Mn 3d level. The weak band located at about 903 nm can be assigned to spin-forbidden transitions of an electron from e_g orbital to t_{2g} orbital of Mn^{2+} ($3d^5$) ions. Photoluminescence (PL) spectra shows that the three characteristic emission band at around 415 nm, 487 nm and 505 nm for pure $MnWO_4$ ascribes the intrinsic optical behaviour of the host system. The oxidation state of manganese (Mn) and gadolinium (Gd) were investigated using electron paramagnetic resonance (EPR) spectroscopy.

1. INTRODUCTION

When compared to traditional binary oxides (e.g. TiO_2, ZnO and SnO_2 etc.,), multi-metal oxide semiconductors possess higher tolerance to structural distortion due to their inherent lattice strain, which enables the incorporation of foreign ions into the host matrix. The multi-metal oxides show higher chemical stability and fewer electron-hole pair recombination centers, so that charge carrier separation and migration is more effective. Bimetallic compound materials belonging to the tungstate and molybdate families have a long history of practical applications and have been the object of extensive research over the past century.

Tungstates and molybdates with a general formula of AWO_4 mainly form two different structures such as Scheelite and Wolframite which is directly related to the bivalent cation size. If the ionic radius of the cations are rA^{2+} < 0.77 Å (for example, Fe, Mn, Co, Ni, Mg, Zn), the materials form the wolframite structure, where the tungsten (or molybdenum) atom adopts an overall 6-fold coordination. Bivalent cations with larger size of rA^{2+} > 0.99 Å design the sheelite structure where the tungsten ions placed a tetrahedral coordination within oxygen-ion cages. These metal tungstates are the important family of inorganic, electro optic materials. Their distinct structure is associated with interesting physical properties such as excitonic luminescence, thermo luminescence, and Stimulated Raman scattering (SRS).

Numerous interests in these compounds lie in their excellent optical properties, which form the basis of their wide use as phosphors, laser materials and scintillation detectors.[1] Especially, metal tungstates are attractive materials and have received great research interest due to their intriguing luminescence and structural properties.

Magnetoelectric multiferroics have attracted renewed interest due to the cross coupling between magnetic and ferroelectric orders as well as potential applications in magnetic sensors, multi-state memories and spintronic devices, etc.[2,5] Recently, large magnetoelectric effects have been observed in so-called type-II multiferroics, in which ferroelectric polarization is induced by non-centrosymmetric magnetic order.[6] One of the common features in this type of multiferroics is that ferroelectric polarization arises from specific spin orders via spin-correlated mechanisms, in particular in noncollinear cycloidal spin order through the inverse Dzyaloshinskii–Mariya (DM) interaction mechanism or E-type antiferromagnetic order through the symmetric exchange striation.[7,10] In order to deeply understand the coupling mechanism and optimize magnetoelectric effects, the multiferroic properties of type-II multiferroics have been extensively studied by modifying their exchange

interaction, since the magnetic structure plays a key role in determining the ferroelectric properties. Among these type-II multiferroics, $MnWO_4$ is a representative and well-studied compound.[8,10] It is monoclinic with space group P2/c and each unit cell includes two Mn^{2+} ions that are interconnected by edges of distorted MnO_6 octahedra, forming zigzag chains along the c axis. The W^{6+} ions stacking alternately along the a axis are also coordinated by oxygen octahedral, corners sharing with MnO_6 octahedral. Besides, this compound shows a complicated magnetic structure, which is established out of competition and subtle balance among complicated multiple magnetic interactions.

2. EXPERIMENTAL

Synthesis of pure and Gd doped $MnWO_4$ compounds

$Na_2WO_4.2H_2O$, $Gd(CH_3COO)_3$ and $MnCl_2.6H_2O$ obtained from Alfa Aesar, USA, were used as precursors for the synthesis of the manganese tungstate ($MnWO_4$) and Gd doped $MnWO_4$ compounds. Synthesis of $MnWO_4$ was carried out by reacting a well-ground mixture of $MnCl_2$ and Na_2WO_4 in a molar ratio of 1:1. Sample mixtures were put into crucibles and then exposed to domestic microwave operating at frequency of 2.45 GHz and a power of 1100 W for 15 min duration. The obtained samples were washed with distilled water to remove the sodium chloride reaction by product and dried at 90°C. Synthesis of various mole concentration (1 to 5 mole %) Gd doped $MnWO_4$ compounds were carried out in a similar manner by reacting to a well-ground mixture of Na_2WO_4, $Gd(CH_3COO)_3$ and $MnCl_2$, as mentioned above. Synthesis of manganese tungstate ($MnWO_4$) and Gd doped $MnWO_4$ compounds were according to the following chemical reactions:

$Na_2WO_4 + MnCl_2 \rightarrow MnWO_4 + NaCl$

$Na_2WO_4 + MnCl_2 + (1 \text{ to } 5 \text{ mole } \%)\ Gd(CH_3COO)_3 \rightarrow MnWO_4{:}Gd + NaCl$

3. RESULT AND DISCUSSION

3.1 XRD analysis

Figure 1 (a-f) shows the XRD patterns for the synthesised pure and Gd doped $MnWO_4$ tungstates. The unit cell parameters were calculated from the powder X-ray diffraction data using CRYSFIRE software. The calculated structural parameters are given in Table-1. The indexed diffraction peaks could be ascribed to a monoclinic structure of $MnWO_4$ with lattice constants of a = 4.80 Å, b = 5.71 Å and c = 4.97 Å, respectively. All diffraction peaks and calculated structural parameters are in good agreement with those in the Joint Committee on Powder Diffraction Standards (JCPDS) card no. 72-0478. The pattern of pure and Gd doped

$MnWO_4$ indicates the main diffraction peaks of monoclinic $MnWO_4$ phase at 2θ = 23.5°, 29.7°, 31.01°, 35.9°, 40.2°, 44.3°, 44.7°, 57.3°, 65.9° and 75.7° which correspond to the (011), (111), (020), (002), (102) (211), (221), (300), (045) and (431) crystallographic planes, respectively. As Figure 1 reveals, no characteristic peaks from non-reacting starting materials are detected on the XRD patterns of the synthesised $MnWO_4$ tungstates, indicating that the products obtained are single phase materials. With the doping of Gd no new peak was found due to $Gd(CH_3COO)_3$ ascribed the incorporation of Gd into Mn lattice site and the intensity increased and decreased gradually. It was observed that the space group of $MnWO_4$ with different Gd^{3+} ions concentrations are all P2/c. As shown in Figure 1 (b-f), the diffraction peak positions are slightly shifted to a smaller degree with increasing concentration of Gd^{3+}, which can be attributed to the increase of the lattice parameters for the substitution of smaller sized Mn^{2+} (ionic radius = 0.08 nm) by the larger sized Gd^{3+} (ionic radius = 0.0912 nm) in the $MnWO_4$:Gd^{3+}. Table 1 lists the full width at half maximum (FWHM) values of (020) reflection peak of pure and Gd doped $MnWO_4$ compounds. The FWHM of the (020) peak of Gd doped $MnWO_4$ higher than that of pure $MnWO_4$ due to may be crystal lattice strain occur in Gd doped $MnWO_4$. In conformity, the average crystalline size of the pure and Gd doped $MnWO_4$ assessed using Scherrer's equation [$D = 0.9\ \lambda/\beta\ \cos\theta$: where β is the FWHM of the diffraction line in radians and λ is the X-ray wavelength] based on using the (020) reflection at 31.01°. The average crystalline size of the pure and $MnWO_4$ compound could be determined by employing the Scherrer's formula and it was found to be 852-1100 nm.

Table 1: FWHM, structural parameters and crystalline size of pure and Gd^{3+} doped $MnWO_4$ compounds.

Compounds	Lattice parameters (Å)			Volume (V) $(Å)^3$	Density (D) (g/cm^3)	FWHM of GAXRD peak (020) (deg.)	Crystalline size (nm)
	a	b	c				
Pure $MnWO_4$	4.80	5.71	4.97	137	382.3	0.02847	852
1 mole % Gd^{3+} doped $MnWO_4$	4.81	5.70	4.98	138	383.1	0.02893	914
2 mole % Gd^{3+} doped $MnWO_4$	4.81	5.69	4.98	140	384.2	0.02900	989
3 mole % Gd^{3+} doped $MnWO_4$	4.82	5.69	4.99	144	385.1	0.02921	1034
4 mole % Gd^{3+} doped $MnWO_4$	4.83	5.68	4.99	146	385.3	0.02978	1081
5 mole % Gd^{3+} doped $MnWO_4$	4.84	5.67	4.99	147	386.2	0.03023	1100

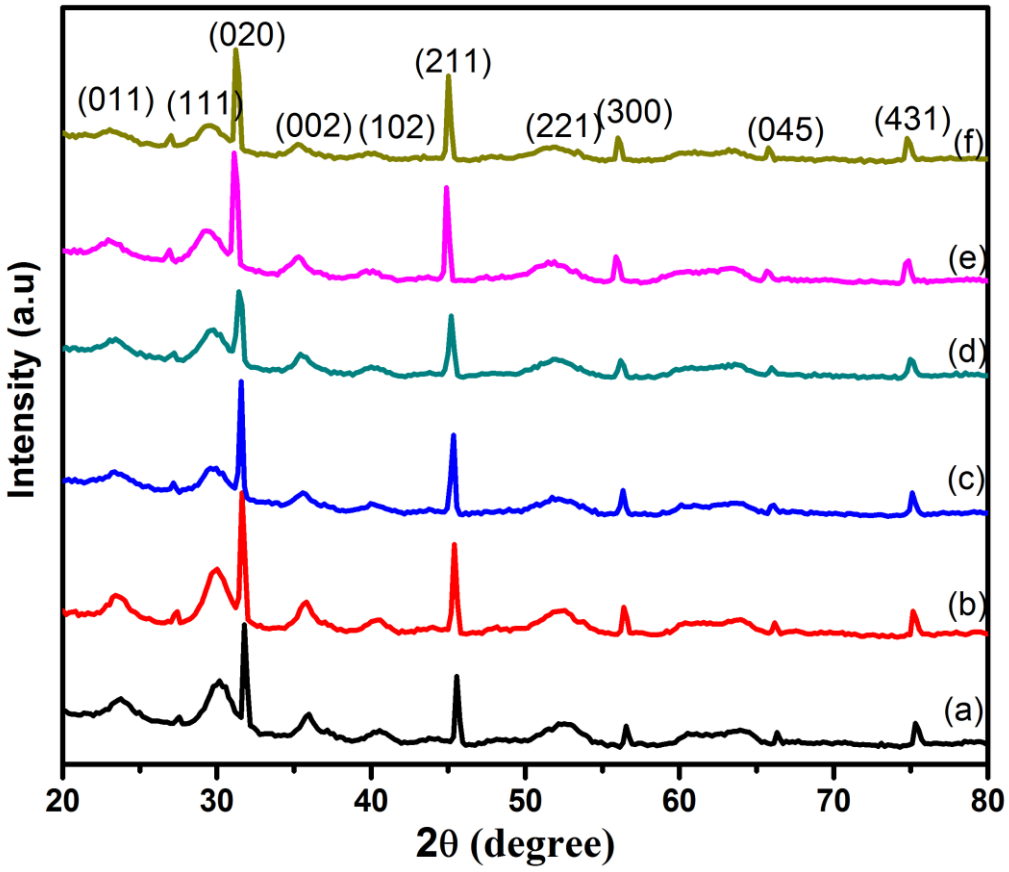

Figure 1(a-f): Powder XRD spectra of (a) pure $MnWO_4$ (b) 1 mole % (c) 2 mole % (d) 3 mole % (e) 4 mole % (f) 5 mole % Gd^{3+} doped $MnWO_4$.

3.2 UV-Visible Spectral Studies

It is well accepted that the optical absorption measurement was one of the most widely used techniques for confirm the substitution of dopant into host lattice. At the same time the change in electronic band structure also can be identified using UV-Vis absorption spectra. The UV-Vis absorption spectra of synthesised pure and Gd doped $MnWO_4$ compounds are shown in Figure 2. The strong absorption maximum of ~359 nm was observed for all the samples. Due to the high crystallinity the samples have shown more prominent UV absorption maxima. The strong band located at about 359 nm can be assigned to the intense band to band transition corresponding to the absorption between the O 2p level and Mn 3d level. The weak band located at about 903 nm can be assigned to spin-forbidden transitions of an electron from e_g orbital to t_{2g} orbital of Mn^{2+} ($3d^5$) ions. There was no additional absorption due to the Gd was seen in the UV-Vis spectra, demonstrate the substitution of Gd into Mn lattice. By the addition of Gd only the small shift in the absorption band was observed towards lower wavelength for the samples. This may be due to the active interaction

of trivalent cation with divalent ions. The absorption peak at ~359 nm does change significantly whereas peak broadening decreases in magnitude, possibly due to the formation of wide distribution of Gd ions in the wolframite structure of $MnWO_4$ compound. The strong d-d transition band was observed in the far-visible regions ~ 1449 nm corresponds to the d-d transition of Mn^{2+} ions in $MnWO_4$ system, which also shifted slightly towards lower wavelength with respect Gd doping concentration.

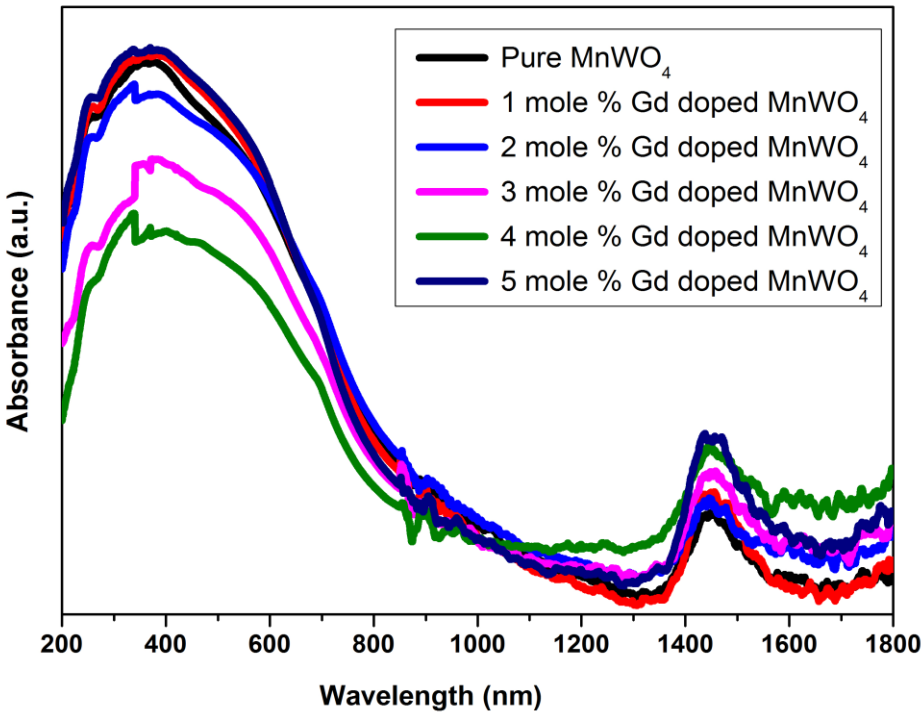

Figure 2: UV-Vis absorption spectra of pure and Gd-doped $MnWO_4$.

3.3 Photoluminescence (Pl) Studies

Figure 3 shows typical room temperature photoluminescence (PL) spectra of pure and Gd doped $MnWO_4$ compounds. From the figure it can be seen that the three characteristic emission band at around 415 nm, 487 nm and 505 nm for pure $MnWO_4$ compound ascribes the intrinsic optical behaviour of the host system. The luminescent efficiency seems to be closely related to the process of synthesis for obtaining particles that are not agglomerate but well formed crystals. In comparison of the pure $MnWO_4$ compound and with the 4 and 5 mole % Gd doped $MnWO_4$ exhibit a red shift to higher wavelength region in the emission band, with decrease in the intensity. The shift in emission band to higher wavelength might be related to the nature of variation of band gap. It is noticeable in the PL spectra the sudden drop in the intensity at doping Gd (4 and 5 mole %) concentration demonstrates that the small to large amount of Gd acts as the luminescent killer in the $MnWO_4$ matrix. Thus severe

luminescent quenching was observed all concentration of Gd doping $MnWO_4$ compounds. As can be seen from the figure there is no other band related to the Gd has been observed even high concentration further confirms the complete incorporation of Gd in Mn lattices. Absence of deep level visible emission in PL spectra confirms the defect free crystalline nature of the pure $MnWO_4$ compound.

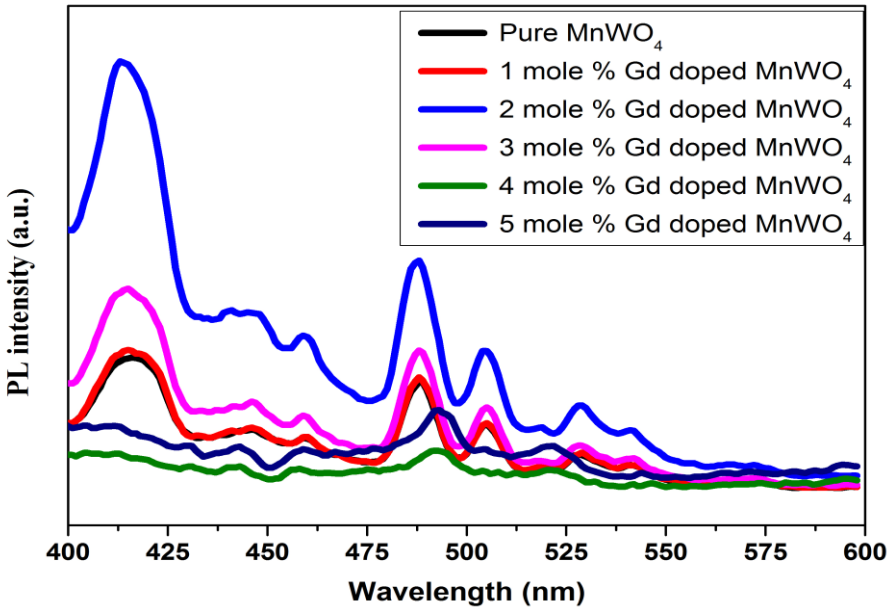

Figure 3: Photoluminescence spectra of pure and Gd-doped $MnWO_4$.

3.4 Scanning electron microscopy (SEM) and Energy Dispersive X-Ray (EDAX) Analysis

Figure 4 (a-f) represents the SEM micrographs for pure and Gd-doped MnWO4 compounds. From the SEM images it can be seen the more information on the grains and nature of the samples. Captured SEM images clearly show the formation of self-aggregated particles, highly homogeneous and cubical in shape. It is clearly seen that the particles are highly aggregated emerged in well crystalline in nature. The addition of Gd into $MnWO_4$ made no changes in the surface morphology except the crystal diameter which is in the range of 850-1100 nm. This result indicates that the addition of Gd retain their microstructure without altering the crystalline structure and morphology. With increase in the doping concentration the particle size was increased significantly and the uniform particle distribution was also observed. This result further confirms the complete incorporation of Gd on to Mn lattice site.

The quantitative elemental analysis was performed using EDAX directly attached with the SEM analysis. The observed EDAX spectra of pure and 5 mole % Gd doped $MnWO_4$ are

shown in Figure 5 (a-b). The atomic concentration of the primary elements present in the pure and Gd doped $MnWO_4$ compounds are given in Table 1. EDAX spectra obviously designate the presence of functional elements of Mn, Gd, W and O with appropriate concentration without any impurities which confirms the stochiometric concentration of the elements. From Table 1, it can be observed that there is deviation in the compositions of Mn, when the concentration of Gd increases in $MnWO_4$ compounds. The results indicate that Gd might act as a substitute at the Mn site in the $MnWO_4$ compound system.

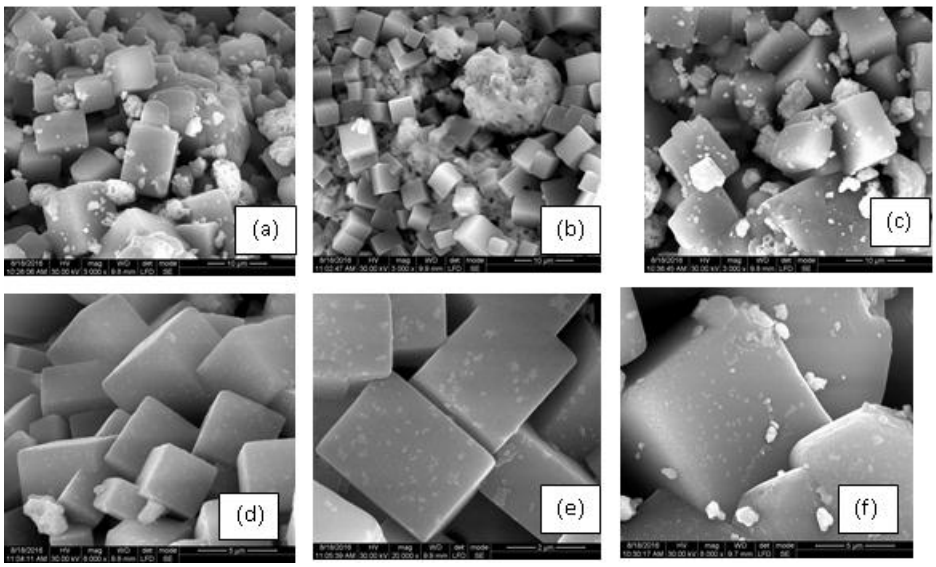

Figure 4(a-f): SEM images of (a) pure $MnWO^4$ (b) 1 mole % (c) 2 mole % (d) 3 mole % (e) 4 mole % (f) 5 mole % Gd^{3+} doped $MnWO_4$.

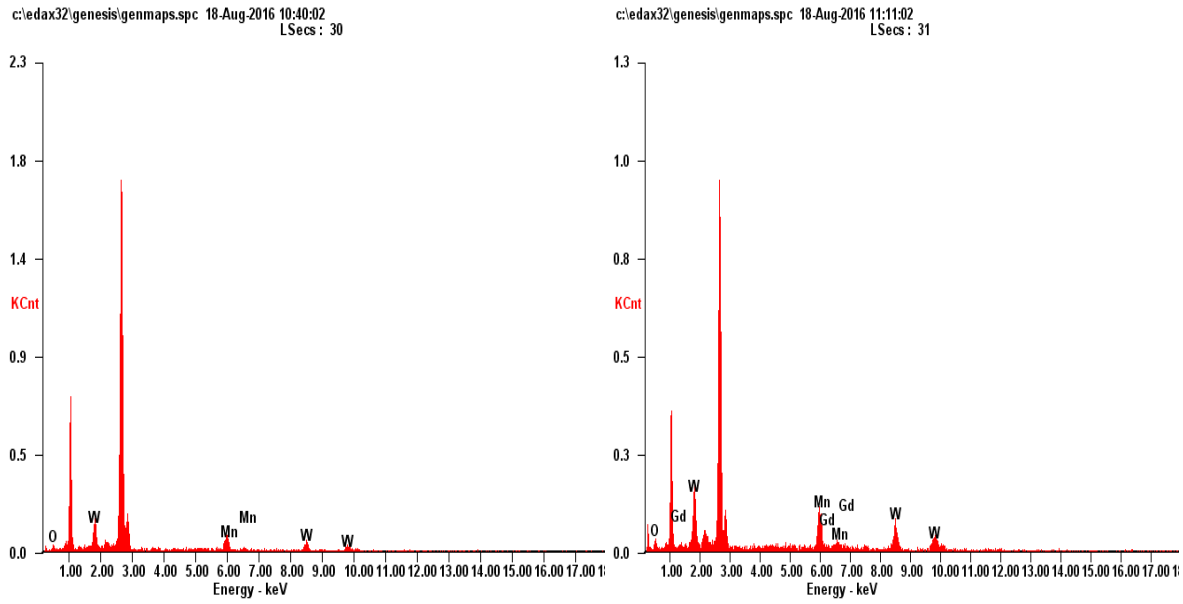

Figure 5 (a-d): EDAX spectra of pure (a) and 5 mole % Gd doped $MnWO_4$ (b).

3.5 Raman spectra analysis

$MnWO_4$ is crystallized in a wolframite structure, which belongs to monoclinic space group P2/c and C_{2h} point-group with two formula units per primitive cell. By making the correlation between site group and factor group for each site, and then eliminating the acoustic mode, we obtain the vibrational modes of $MnWO_4$: $\Gamma_{(k=0)} = 8A_g + 10B_g + 7A_u + 9B_u$ lattice translational modes of the Mn^{2+} and W^{6+} ions. Internal modes can be subdivided into $3A_g + 3B_g$ symmetric stretching (ν_s (W–O–W)) and symmetric bending (ν_s (W–O–W)) vibrations of the double W-O-O-W oxygen bridge, $3A_u + 3B_u$ anti-symmetric stretching (ν_{as} (W–O–W)) and antisymmetric bending (ν_{as} (W–O–W)) vibrations of the double W-O-O-W oxygen bridge modes, $A_g + A_u$ ($B_g + B_u$) symmetric (antisymmetric) stretching of the WO_2 groups (ν_s (WO_2) and ν_{as} (WO_2)), $A_g + A_u$ scissoring ($\delta_{sc}(WO_2)$), $B_g + B_u$ rocking ($\rho(WO_2)$), $A_g + A_u$ twisting ($\tau(WO_2)$) and $B_g + B_u$ wagging modes ($\omega(WO_2)$). Selection rules, show that all g modes ($8A_g + 10B_g$) are Raman active and all u modes ($7A_u + 8B_u$) are IR active. Figure 6 shows polarized Raman spectra of $MnWO_4$ obtained at room temperature. All Raman modes are strongly polarized, some of the A_g modes are shown weakly in the spectra where they are forbidden, and vice versa. It should be noted that the B_g mode at 200 cm^{-1} can be observed. The internal vibration modes associated with W-O bonds of the WO_6 octahedra from those associated with Mn-O bond in between the octahedral. This is reasonable since the strong electro negativity of hexavalent tungsten would result in highly covalent W-O bond than the more ionic Mn-O bond. No additional bands are observed which could be attributed to Gd based impurity phase. This result confirms that the studied crystal are homogenous (i.e) there is no phase separation into $MnWO_4$ and Gd based phases but Gd^{3+} substituted for Mn^{2+} in the wolframite-type structure. The internal modes of the pure and Gd doped $MnWO_4$ are listed in Table 2. From the Raman spectra, when the Gd concentration were increased the high intense peak at 885 cm^{-1} intensity decreases and also lower Raman wavenumber not followed in higher concentration Gd doped $MnWO_4$. This result indicates that substitution of Gd^{3+} for Mn^{2+} induced some weak changes in the bond lengths and angles of the wolframite-type structure due to higher ionic size of the Gd^{3+} ions (0.912 Å) when compared to the ionic radius of Mn^{2+} ions (0.83 Å). This result can be attributed to substitutional disorder induced by concentration of dopant ions in the $MnWO_4$ lattice.

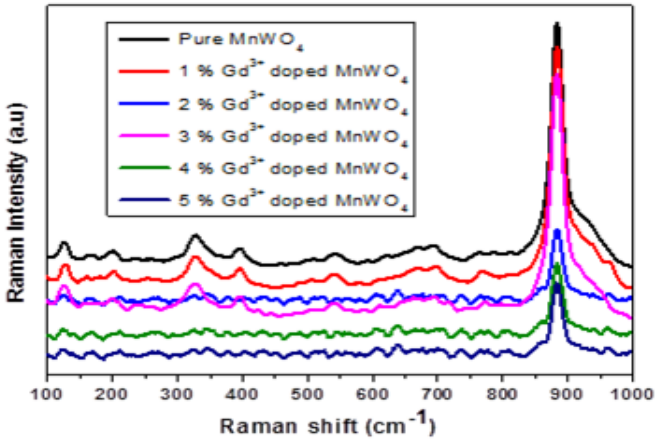

Figure 6: Raman spectra of pure and Gd^{3+} $MnWO_4$.

Table 2: Raman wavenumbers of pure and Gd^{3+} doped $MnWO_4$ together with the proposed assignment.

Pure $MnWO_4$	1 % Gd doped $MnWO_4$	2 % Gd doped $MnWO_4$	3 % Gd doped $MnWO_4$	4 % Gd doped $MnWO_4$	5 % Gd doped $MnWO_4$	Assignment
885 (strong)	885 (strong)	885 (strong)	885 (medium)	885 (medium)	885 (medium)	$\nu_s(WO_2)$
772	772	772	772	772	772	$\nu_{as}(WO_2)$
696	696	696	696	696	696	ν_s(W-O-W)
544	544	544	544	544	544	ν_s(W-O-W)
396	396	396	396	396	396	ν_s(W-O-W)
326	326	326	326	326	326	$\nu_{sc}(WO_2)/\nu_s$(W-O-W)
200	200	200	200	200	200	$\rho(WO_2)$
126	126	126	126	126	126	$\omega(WO_2)$

3.6 FT-IR spectra studies

FT-IR spectra of the synthesized pure and Gd doped $MnWO_4$ are shown in Figure 7. A broad band observed at 3414 cm^{-1} is indicative of vibration of O–H bond of the surface hydration. The band at 1638 cm^{-1} corresponds to the H–O–H deformation vibration of surface hydroxyl group. The absorption peaks located at 1419 cm^{-1} and 837 cm^{-1} corresponds to symmetric and asymmetric stretching vibration mode of the W–O bond in terminal WO_2 group of $MnWO_4$. The weak band at 711 cm^{-1} is the asymmetrical stretching vibrations of W–O bond in the $(W_2O_4)_n$ chain and 607 cm^{-1} indicates the presence of stretching vibration of Mn–O bond. When Gd doped $MnWO_4$ does not change the band position.

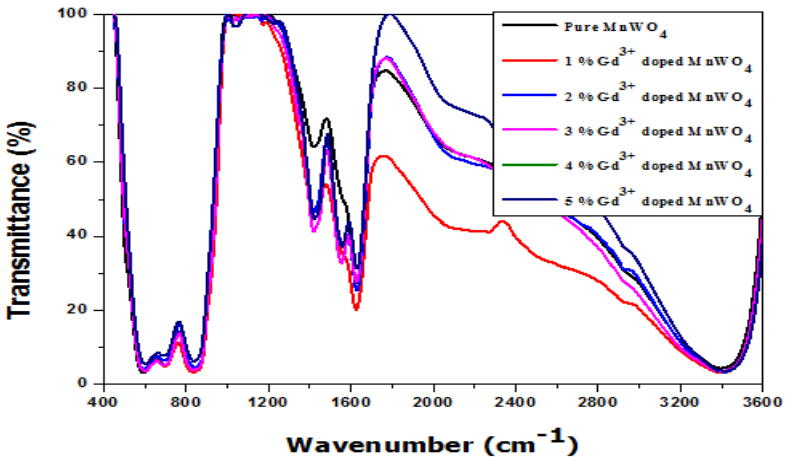

Figure 7: FTIR spectra of pure and Gd^{3+} doped $MnWO_4$.

3.7 Electron paramagnetic resonance (EPR) studies

Electron paramagnetic resonance (EPR) analysis was carried out in order to confirm the oxidation state of Mn ion present in $MnWO_4$. Figure 8 shows the curve that corresponds to a signal produced due to the presence of ferromagnetic Mn^{2+} ions. The observed EPR signal was justified by the g factor, that is

$g = h\nu/\beta H$

Where g is a parameter describing the interaction of the paramagnetic center with the external magnetic field, h is the Planck's constant, ν is the microwave frequency, β is the Bohr Magneton and H is the intensity of the resonance magnetic field. The value of g was found to be 2.0017 which is typical of octahedral environment of Mn^{2+}. From EPR analysis the oxidation state of Mn present in $MnWO_4$ was found to be Mn^{2+}. The g value and EPR peak position does not changed in Gd doped $MnWO_4$.

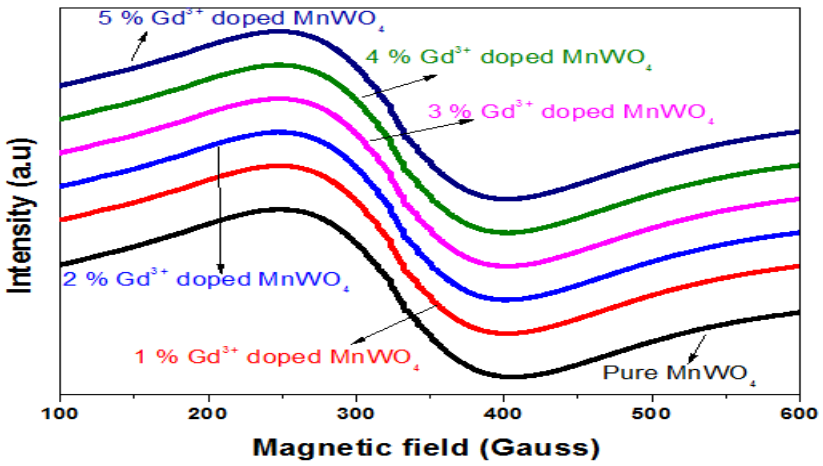

Figure 8: EPR spectra of pure and Gd^{3+} doped $MnWO_4$.

3.8 Thermal analysis of the pure and Gd doped $MnWO_4$

Thermogravimetric analysis (TGA) and differential thermal analysis (DTA) was conducted to check the thermal stability and crystalline condition of the as prepared pure and Gd doped $MnWO_4$. The pure and Gd doped $MnWO_4$ sample were heated from RT to 1200°C with a successive increment of 10°C per minute in nitrogen atmosphere. Figure 9 (a-c) curve red line and blue line shows the TGA and DTA curve of pure, 3 mole % Gd and 5 mole % Gd doped $MnWO_4$, respectively. From curve red line, upto 800°C does not occur weight loss it may be indicates the moisture or adsorbed water molecule not present in these samples. The DTA analysis in curve blue line shows strong one endothermic peaks located at 769, 763 and 763°C appear for pure, 3 mole % Gd and 5 mole % Gd doped $MnWO_4$, respectively.

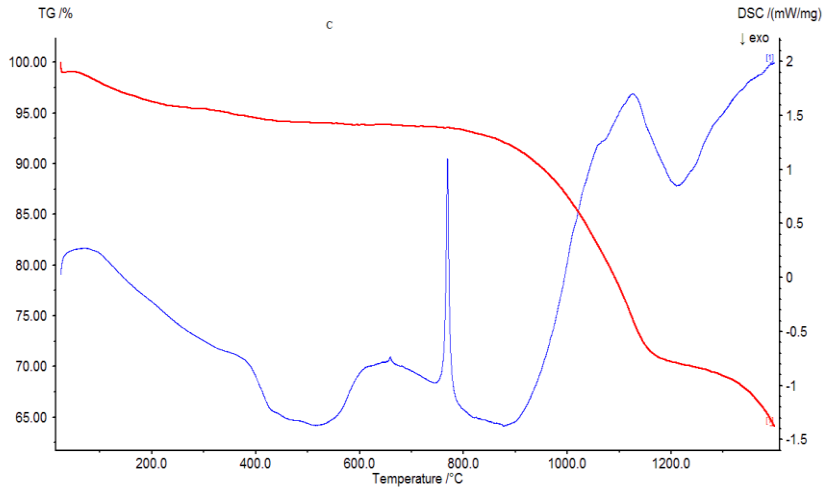

Figure 9a: Curve red line and blue line shows the TGA and DTA curve of $MnWO_4$.

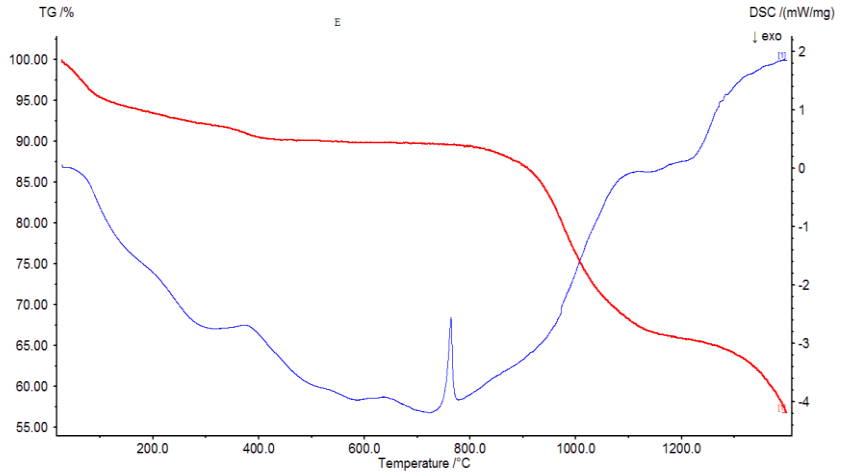

Figure 9b: Curve red line and blue line shows the TGA and DTA curve of 3 mole % Gd^{3+} doped $MnWO_4$.

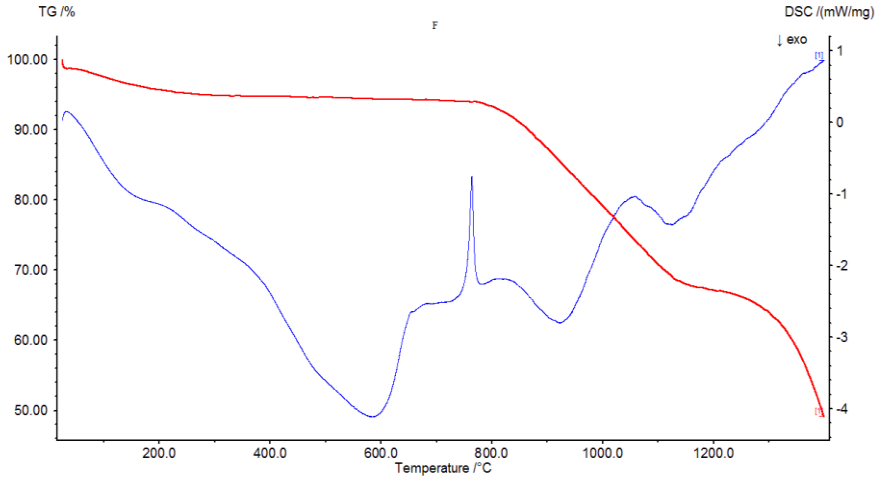

Figure 9c: Curve red line and blue line shows the TGA and DTA curve of 5 mole % Gd^{3+} doped $MnWO_4$.

4. CONCLUSION

Novel solid state metathesis approach has been employed to synthesis technologically important pure and Gd doped $MnWO_4$ materials. The X-ray diffraction analysis clearly shows that the Gd doped $MnWO_4$ compounds are single phase in the monoclinic (wolframite) structure. Optical absorption edge energies for the pure and Gd doped $MnWO_4$ synthesised in this study have been determined. UV-Vis absorption analysis of pure Gd doped exhibits the intense UV absorption at 359 nm which confirms the excellent optical behaviour of the monoclinic (wolframite) structure. The small wavelength shift was towards lowering wavelength region for the doped samples addressing the interaction of Gd^{3+} ion with $MnWO_4$ structure. When SEM showed will-defined morphology for pure and Gd doped $MnWO_4$ prepared by this method, which have distinct advantages in terms of simplicity, easy scale up and are relatively inexpensive with high yield. The phonons in pure and Gd doped $MnWO_4$ are studied by means of Raman scattering spectra.

REFERENCES

1. K. Naik, A. Gangan (Facile Hydrothermal Synthesis of $MnWO_4$ Nanorods for Non-Enzymatic Glucose Sensing and Supercapacitor Properties with Insights from Density Functional Theory Simulations) Chemistry Select', 2017; 2: 5707-5715.
2. Do Dang Trung, Nguyen Duc Cuong, Khuc Quang Trung, Thanh-Dinh Nguyen (Controlled synthesis of manganese tungstate nanorods for highly selective NH_3 gas sensor) Journal of Alloys and Compounds, 2018; 735: 787-794.

3. Mostafa Khaksar, Davar M. Boghaei, Mojtaba Amini (Synthesis, structural characterization and reactivity of manganese tungstate nanoparticles in the oxidative degradation of methylene blue) Comptes Rendus Chimie, 2015; 18;2: 199-203.
4. Yonggang Wang, Linlin Yang, Yujiang Wang, Xiaofeng Wang, Gaorong Han (Morphology-controlled synthesis and characterization of $MnWO_4$ nanocrystals via a facile, additive-free hydrothermal process) Journal of Alloys and Compounds, 2016; 654: 246-250.
5. Jan Ungelenk, Sabine Roming, Peter Adler, Walter Schnelle (Ultrafine $MnWO_4$ nanoparticles and their magnetic properties) Solid State Sciences, 2015; 46: 89-94.
6. M.A.P. Almeida, L.S. Cavalcante, J.A. Varela, M. Siu Li, E. Longo (Effect of different surfactants on the shape, growth and photoluminescence behavior of $MnWO_4$ crystals synthesized by the microwave-hydrothermal method) Advanced Powder Technology, 2012; 23: 124-128.
7. G.G. Fouga, R.M. Taddeo, M.V. Bosco, A.E. Bohé (Kinetic study of Hubnerite ($MnWO_4$) chlorination) Thermochimica Acta, 2012; 536: 30-40.
8. H. Ehrenberg, H. Weitzel, H. Fuess (Magnon dispersion and magnetic phase diagram of $MnWO_4$) Physica B: Condensed Matter, 1997; 234–236; 560-563.
9. M.A.K.L. Dissanayake, O.A. Ileperuma, P.A.G.D Dharmasena. (A.C. conductivity of $MnWO_4$) Journal of Physics and Chemistry of Solids, 1989; 50: 359-361.
10. Hongjun Zhou, Yuen Yiu, M.C. Aronson, Stanislaus S. Wong (Ambient template synthesis of multiferroic $MnWO_4$ nanowires and nanowire arrays) Journal of Solid State Chemistry, 2008; 181: 1539-1545.